

# DEM Analyses with the Utrecht Codes

R. MEWE,<sup>1</sup> G. H. J. VAN DEN OORD,<sup>2</sup>  
C. J. SCHRIJVER,<sup>3</sup> AND J. S. KAASTRA<sup>1</sup>

<sup>1</sup>SRON Laboratory for Space Research, Sorbonnelaan 2, 3584 CA Utrecht, The Netherlands

<sup>2</sup>Sterrekundig Instituut Utrecht, P.O. Box 80 000, 3508 TA Utrecht, The Netherlands

<sup>3</sup>Stanford/Lockheed Inst. for Astrophys. and Space research, LPARL,  
Dept. 91-30, Bldg. 252, 3251 Hanover Street, Palo Alto, CA 94304-1191, USA

We address the inversion problem of deriving the differential emission measure (DEM) distribution  $D(T) = n_e n_H dV/d \log T$  from the spectrum of an optically thin plasma. In the past we have applied the iterative Withbroe-Sylwester technique and the Polynomial technique to the analysis of *EXOSAT* spectra of cool stars, but recently we have applied the inversion technique discussed by Craig & Brown (1986) and Press et al. (1992) in the analysis of *EUVE* spectra of cool stars. The inversion problem—a Fredholm equation of the first kind—is ill-posed and solutions tend to show large, unphysical oscillations. We therefore apply a second-order regularization, i.e., we select the specific DEM for which the second derivative is as smooth as is statistically allowed by the data. We demonstrate the importance of fitting lines and continuum *simultaneously*, discuss the effect on the DEM of continuum emission at temperatures where no line diagnostics are available, and address possible ways to check various model assumptions such as abundances and photon destruction induced by resonant scattering.

## 1. Introduction

The X-ray spectrum of optically thin sources contains contributions from plasmas at different temperatures as is indicated by the presence of lines which have different formation temperatures. The underlying continuum emissivity is a slowly varying function of the plasma temperature and varies as  $\sim \exp(-hc/\lambda kT)/\sqrt{T}$ . Hence, at temperatures  $kT \gtrsim 2hc/\lambda$  the shape of the continuum does not vary significantly making it a poor temperature probe. For the analysis of *EUVE* spectra this causes problems for  $T \gtrsim 20$  MK because at these temperatures only few lines are present, while the continuum cannot be used to constrain  $T$ . Though the continuum is of limited use as a diagnostic at high temperatures, it is of paramount importance for the spectral analysis as a whole. Spectral fitting based on only line emission can give erroneous results. We show this with a straightforward example: the effect of non-standard abundances in a source. Suppose an observed spectrum contains a number of dominant Fe lines. When the emissivity of each line is known one can assign an emission measure to each line corresponding to the formation temperature of the line. The result is, however, based on the *assumed* Fe abundance: if this is too high the derived emission measures will be too low. The check which can be made is to see whether the emission measures derived for the lines result in an acceptable fit to the continuum. If the assumed abundances are too high, and the derived emission measure as a consequence too low, the theoretically calculated continuum will be below the observed continuum signalling that there is something wrong with the assumed model. This simple example demonstrates the importance of fitting both lines and continuum simultaneously.

How accurately can we recover the temperature distribution of the source plasma using the spectral lines as temperature probes? The formation process of a spectral line depends on the ionization balance and on the excitation process, which both depend on temperature. As a result, the temperature information is spread out over a typical

width  $\sigma_T$  over which the line is formed and which is generally roughly a factor two in temperature, i.e.,  $\log \sigma_T \approx 0.3$ . This corresponds to an intrinsic limit for the temperature resolution which can be achieved, regardless of the resolution of the instrument.

In analyzing the temperature structure of a source from the observed spectrum, one usually introduces the concept of the *differential emission measure* (DEM) which is a weighting function measuring the contribution of the plasma at each temperature to the observed spectrum. We point out a fundamental problem concerning the retrieval of the DEM from an observed spectrum. Suppose the spectrum is observed in  $n$  wavelength bins. The *observed* counts in the bins form the elements of a vector  $\mathbf{g}$ . In a similar way the *expected* counts from a spectral model, at a temperature  $T_j$ , can be represented by a vector  $\mathbf{f}_j$ . Determining the DEM comes down to solving over  $m$  temperature bins:

$$\mathbf{g} = \sum_{j=0}^m D_j \mathbf{f}_j = D_1 \mathbf{f}_1 + D_2 \mathbf{f}_2 + \dots + D_m \mathbf{f}_m,$$

with  $D_j$  the differential emission measure at temperature  $T_j$ . If the vectors  $\mathbf{f}_j$  would constitute an orthogonal set then it would be straightforward to determine the coefficients  $D_j$ . Simply taking the dot product of  $\mathbf{f}_j$  on both sides of the expression would give  $D_j = \mathbf{f}_j \cdot \mathbf{g} / \mathbf{f}_j \cdot \mathbf{f}_j$  since  $\mathbf{f}_j \cdot \mathbf{f}_i = 0$  for  $i \neq j$ . However, in reality the vectors  $\mathbf{f}_j$  do not constitute an orthogonal set which means that *no unique solution exists* for the coefficients  $D_j$ . Each vector  $\mathbf{g}$  can be decomposed into the vectors  $\mathbf{f}_j$  in an infinite number of ways. Additional information has to be provided to select a  $D_j$  from the infinite set of solutions. Exempli gratia, for a one-temperature fit one provides the information that the DEM is a delta-function which restricts the number of solutions to the  $m$  values for  $D_j$  determined from  $D_j = \mathbf{f}_j \cdot \mathbf{g} / \mathbf{f}_j \cdot \mathbf{f}_j$ . Amongst these  $m$  values the one is selected which best satisfies a quality criterion for the fit, e.g.,  $\chi^2$ . In general, spectral fitting is based on a combination of assumptions about the expected solution and a quality criterion for the fit.

Since detectors cover only a finite wavelength range one can in principle only obtain information about the differential emission measure in the temperature range for which spectral lines can be observed within the wavelength range of the detector. We note that the *absence* of a specific line in an observed spectrum provides information for the DEM that is as relevant as the *presence* of lines. The continuum, however, contains information from a much broader temperature range than the lines. In other words, the emission measure associated with the continuum does not have to correspond necessarily to the emission measures derived from the lines. This limits the use of the continuum as a check for, e.g., abundance variations. There is a way out: use a complementary instrument which can observe at higher or lower energies to see whether other temperature components are present in a source. These components can then be responsible for an 'excess' continuum at the observed wavelengths but for which no line diagnostics are available. If the presence of other components is not confirmed, the continuum can be used for checking the basic model assumptions.

Various inversion techniques exist to recover a DEM distribution over the range of temperatures for which the instrument is sensitive, using optically thin model spectra, convolved with an appropriate instrument response (cf., Thompson 1991).

In the past we have applied an iterative deconvolution technique that was based on a weighting-factor method originally proposed by Withbroe (1975), modified later by Sylwester et al. (1980): the Withbroe-Sylwester (WS) method. The technique is formulated to exclude a priori negative values for the emission measure. It makes no assumptions about the functional form of the DEM, although the final result is subject to an implicit smoothing, because the weighting functions contain integrals over the entire spectral

range. It was applied to the analysis of X-ray spectra of solar flares and to spectra of several cool stars measured with the transmission grating spectrometer (TGS) on board *EXOSAT* (Lemen et al. 1989). Lemen et al. also used the Polynomial (P) method, which assumes that the DEM can be approximated by  $\mathbf{D}(T) = \alpha \exp[\omega(T)]$ , where  $\omega(T)$  is a polynomial function of temperature for which a sum of Chebyshev polynomials was chosen allowing any arbitrary functional form for the DEM to be approximated as the number of terms in the sum is increased. In the *EXOSAT* analysis they have used polynomials of order 9. This technique also precludes negative values for the DEM. Recently we have developed the software—built into our new spectral code SPEX—for an inversion technique as discussed by Craig & Brown (1986) and by Press et al. (1992) which uses a matrix inversion by singular-value matrix decomposition combined with second-order regularization and which has been applied to the analysis of *EUVE* spectra of cool stars.

## 2. Inversion by Statistical Regularization

Spectra emitted by optically thin coronae are linear combinations of isothermal spectra and are interpreted as statistical realizations of models calculated with our code for optically thin plasmas. In our models we assume (thermal) collisional ionization equilibrium, thus ignoring possible transient effects, and we ignore effects that depend on the plasma density, which affect only a few lines. Let an isothermal plasma of temperature  $T$  emit a spectrum that, when incorporating interstellar absorption, instrumental efficiencies, and instrumental smoothing, is represented by  $\mathbf{f}(\lambda_i, T_j)$  in a linear grid of wavelength bins of width  $\Delta\lambda$  ( $i = 1, \dots, n$ ) and a logarithmic grid of temperature intervals of width  $\Delta \log(T)$  ( $j = 1, \dots, m$ ), where  $\mathbf{f}(\lambda_i, T_j)$  is the plasma emissivity per unit  $n_e n_H$ . For a composite plasma with temperatures ranging from  $T_1$  up to  $T_m$ , the net expected spectrum  $\mathbf{g}(\lambda_i)$  is given by:

$$\mathbf{g}(\lambda_i) = \int \mathbf{f}(\lambda_i, T) n_e(T) n_H dV(T) \approx \sum_{j=1}^m \mathbf{f}(\lambda_i, T_j) \mathbf{D}(T_j) \Delta \log(T). \quad (2.1)$$

Eq. (2.1) constitutes a Fredholm equation of the first kind for the differential emission measure  $\mathbf{D}(T) = n_e n_H dV/d \log T$  and can be written as a vector equation:  $\mathbf{g} = \mathbf{F} \cdot \mathbf{D}$ , in which  $\mathbf{F}$  is a matrix with  $m$  columns and  $n$  rows, of which the elements are given by  $\mathbf{F}_{ij} = \int_{\lambda_i}^{\lambda_i + \Delta\lambda} \mathbf{f}(\lambda, T_j) d\lambda \Delta \log T \equiv \mathbf{f}_i(T_j) \Delta \log T$ . Each column of  $\mathbf{F}_{ij}$  consists of a ‘spectral’ vector containing the discretized spectrum at a certain temperature. The formal least-squares solution of this problem requires an inversion of

$$\mathbf{F}^T \mathbf{F} \cdot \mathbf{D} = \mathbf{F}^T \cdot \mathbf{g}, \quad (2.2)$$

in which  $\mathbf{F}^T$  is the transpose of  $\mathbf{F}$ . The terms  $[\mathbf{F}^T \mathbf{F}]_{ij}$  are proportional to dot products  $\mathbf{f}_i \cdot \mathbf{f}_j$  while the terms  $[\mathbf{F}^T \mathbf{g}]_j$  are proportional to  $\mathbf{f}_j \cdot \mathbf{g}$ , in which one recognizes the vector decomposition discussed in the introduction. Let  $\tilde{\mathbf{g}}$  represent an observed spectrum which contains noise. The measurement errors are taken into account by introducing a weighting  $\tilde{\mathbf{g}}_i \rightarrow s \tilde{\mathbf{g}}_i / s_i$ ,  $\mathbf{F}_{ij} \rightarrow s \mathbf{F}_{ij} / s_i$  with  $s$  the geometrical mean of the errors. The common practice is then to solve Eq. (2.2) in the classical generalized least-squares sense,  $\|\mathbf{F} \cdot \mathbf{D} - \tilde{\mathbf{g}}\|^2 = \min$ , in which one recognizes the  $\chi^2$ -method. This method does not, however, take into account that information has been lost due to the smoothing action of the kernel in Eq. (2.1). Also, the method forces the solution to fit noisy data points as good as possible, causing high-frequency oscillations in  $\mathbf{D}$ . The way to remedy these problems is to introduce an additional quadratic constraint  $\|\mathbf{R} \cdot \mathbf{D}\|^2$  which reflects some desired property for  $\mathbf{D}$ . One then minimizes a joint functional comprising the

classical  $\chi^2$  constraint and the additional constraint:  $\|\mathbf{F} \cdot \mathbf{D} - \tilde{\mathbf{g}}\|^2 + \varrho \|\mathbf{R} \cdot \mathbf{D}\|^2 = \min$ , where  $\varrho$  is a Lagrangian multiplier commonly referred to as the *regularization parameter* ( $0 \leq \varrho < \infty$ ) which controls the degree of smoothness of the solution. The matrix form of the regularized problem is then given by

$$(\mathbf{F}^T \mathbf{F} + s^2 \varrho \mathbf{R}) \cdot \mathbf{D} = \mathbf{F}^T \cdot \tilde{\mathbf{g}}. \quad (2.3)$$

A suitable choice for the quadratic constraint is *second-order regularization*, given by  $\mathbf{R} \cdot \mathbf{D} = \mathbf{D}''$ , which makes the second derivative as smooth as statistically allowed by the data. The matrix  $\mathbf{R}$  has a band diagonal shape over five columns (see Mewe et al. 1995). Because we use  $\Delta \log T \approx (\log \sigma_T)/3 \approx 0.1$ , the matrix  $\mathbf{R}$  smooths the information over a typical line-formation interval. We note that constraints which require  $\mathbf{D}$  to be positive are too restrictive when the background-subtracted spectra contain bins with only a few, and possibly, negative counts (see Thompson 1991).

When blends occur in an observed spectrum of lines with different formation temperatures, and when a continuum is present in the spectrum, the photon noise together with the imposed smoothing will cause some degree of cross-talk over a temperature range exceeding  $\sigma_T$  resulting in a coupling between different temperature components of  $\mathbf{D}$ . However, in the analysis of the *EUVE* spectra such 'contamination' is limited because the continuum bins have relatively low count rates, corresponding to a low statistical weight, while lines with different formation temperatures are generally well separated.

We stress that the above inversion method is *not* an iterative procedure. An iterative method requires an initial *DEM* distribution, and, depending on the details of the distribution, the iteration may not converge to the true best-fit solution, but instead may yield a solution corresponding to a local minimum in the  $\chi^2$ -space. This problem is avoided by the method discussed in this paper.

### 3. Applications and Examples

A detailed *DEM* analysis using the Mewe et al. (1985, 1986) plasma emission code and the Withbroe-Sylwester (WS) and Polynomial (P) methods was performed on the *EXOSAT-TGS* spectra (5–200 Å) of Capella,  $\sigma^2$  CrB, and Procyon by Lemen et al. (1989). An example of the *DEM* results for Capella is shown in Fig. 2.

For the analysis of the *EUVE* spectra isothermal equilibrium spectra were calculated using our newly developed *SPEX* code, which contains the *MEKA* spectral code, available as a subroutine to the *XSPEC* package, but extended with spectral lines between 300–2000 Å (cf. Kaastra & Mewe 1993, Mewe & Kaastra 1994). The calculated spectra are modified by interstellar absorption using absorption cross sections of Rumph et al. (1994), adopting abundance ratios He I/H I = 0.1, He II/H I = 0.01, and convolved with the instrument response. Solar photospheric abundances from Anders & Grevesse (1989) are used. We have used a range of temperatures between  $3 \cdot 10^4$  K– $10^8$  K divided in 36 logarithmically spaced temperature values (i.e.  $\Delta \log(T) \simeq 0.1$ ). The lower temperature boundary is determined by the presence of strong He II lines which form  $\lesssim 10^5$  K, the upper boundary is chosen well above the highest formation temperature of the lines within the *EUVE* wavelength range. We have chosen a wavelength binning equal to about half the spectral resolution (i.e., 0.25, 0.5, and 1 Å for the SW, MW, and LW, respectively). The emission measure is plotted as  $\mathbf{D}(T)\Delta \log T$  vs.  $\log T$ , with  $\Delta \log T = 0.1$ . The total emission measure in any temperature range can be obtained by summing the values of  $\mathbf{D}(T)\Delta \log T$  over this range.

We have analyzed the spectra of eight late-type stars (cf., Schrijver et al. 1995 and these proceedings), and the pre-main-sequence star AB Dor (cf., Rucinski et al. 1995),



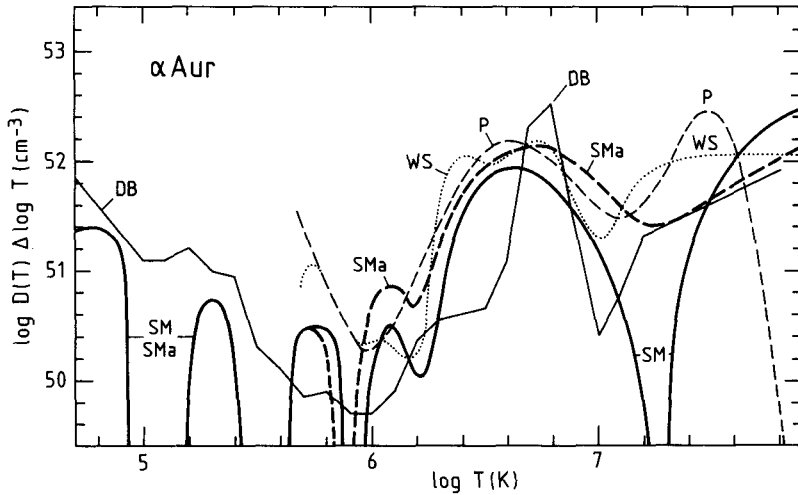


FIGURE 2. DEM curve  $D(T)\Delta \log T$  on a log scale derived by Schrijver, Mewe et al. 1995 for the model with solar abundances from the *EUVE* spectra of Capella (thick solid line, labeled SM) and for the case with Fe abundance  $0.3 \times$  solar (thick dashed line, SMa). For comparison are also drawn the DEM derived by Dupree, Brickhouse et al. (1993) by a DEM analysis from the Capella *EUVE* spectrum (thin solid line, DB) and the *EXOSAT* results derived by Lemen et al. (1989) (thin dotted (WS) and thin dashed (P) lines for the WS and P methods, respectively; original results were multiplied by a factor 2.42 so as to correct for  $n_H/n_e$  and different temperature interval). All curves are for a temperature interval  $\Delta \log T = 0.1$ .

observations which indicate a hot (20–40 MK) component for Capella (cf., Fig. 2). As we discussed in the introduction, the need to add continuum photons can indicate that a plasma component is present in the source at temperatures where no lines form in the *EUVE* wavelength range or it signals that something is wrong with the assumed plasma model. In both cases the high-temperature component in the DEM arises because the values of the DEM required to fit the spectral lines do not generate enough associated continuum photons. To make the fit acceptable any inversion algorithm will add plasma at temperatures where the lines are not influenced. For the *EUVE* this corresponds to temperatures above 20 MK.

More generally, incorrect values for the assumed abundances can be a second cause of a high-temperature component. Line excitation  $\propto n_i n_e$  with  $n_i$  the density of the emitting ions and  $n_e$  the electron density. Continuum emission (predominantly free-free and free-bound emission from H- and He ions) varies proportionally to  $n_e n_H$ . The line/continuum ratio is therefore proportional to  $n_i/n_H$ , the ion abundance, which in turn is proportional to the element abundance. Many of the dominant lines in the *EUVE* spectra, especially in the SW band are from iron. Reducing the Fe abundance will therefore make the continuum relatively stronger with respect to the lines and making it less necessary for the algorithm to invoke a high-temperature component. To illustrate this effect, we also show in Fig. 2 the DEM for a reduced Fe ( $0.3 \times$  solar) abundance (thick dashed line). The high-temperature component is, as expected, reduced in strength while the DEM

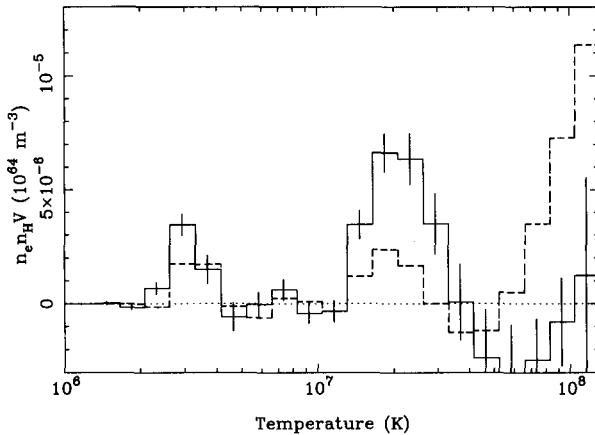


FIGURE 3. Results of a DEM analysis of a simulated *EUVE* spectrum including noise and background subtraction. In the input two-temperature model we take temperatures of 2.9 and 18.4 MK, emission measures of 5 and 15 ( $10^{58} \text{ m}^{-3}$ ),  $d = 12$  pc, exposure time  $10^5$  s and solar abundances except for Fe ( $0.3 \times$  solar). Fitting with  $0.3 \times$  solar Fe abundances recovers the input model (solid line) but when the Fe abundance is incorrectly assumed to be solar (dashed line) a hot component arises above  $\sim 20$  MK to correct the line/continuum ratio.

becomes larger in the  $2 \cdot 10^6 - 10^7$  K range, required to fit the Fe lines when the abundance is lower.

Reduced Fe abundances (in the range  $\sim 0.2-0.4$ ) are probably needed to reconcile *EUVE* observations on Algol (Stern et al. 1995) and AB Dor (Rucinski et al. 1995 and these proceedings) with *ASCA* data, or to explain the re-analyzed *EINSTEIN* SSS spectrum of Capella and the *ASCA* spectrum of AR Lac (e.g., Drake et al. 1994).

To demonstrate the effect of abundances we have simulated an *EUVE* spectrum with noise and typical background subtraction for a model with two temperature delta-functions and solar abundances, except for Fe where we take  $0.3 \times$  solar. If we make a DEM fit with the same model we restore the two components, but when we wrongly assume a solar Fe abundance, indeed a hot component arises above about 20 MK in order to fit the line/continuum ratio with the too large Fe abundance (cf. Fig. 3).

A third explanation for the hot DEM component may be provided by the assumption that we are missing in the spectral code many weaker, closely spaced lines that contribute to and mimic the observed SW continuum such as L-shell lines from the lighter elements (Ne, Mg, Si, S) and Fe M-shell emission (Liedahl, private communication).

A fourth possibility is a non-thermal continuum of comparable strength as the thermal continuum (e.g., Stern et al. 1995) and with a power-law slope similar to a Crab-like spectrum so as to give a flat spectrum on a wavelength scale.

Finally, there is the possibility that the stronger lines are weakened –compared to the optically thin approximation–by the effect of resonant scattering. This effect which is discussed in detail by Schrijver et al. in these proceedings may play a rôle in the coronae of e.g.,  $\alpha$  Cen and Procyon. When a plasma becomes optically thick (optical depth  $\tau \gtrsim 1$ ) the effect on the intensity of a resonance line is determined by the processes competing with the spontaneous radiative decay to the ground level: (1) radiative branching to other

levels, (2) collisional de-excitation, or (3) true absorption in a nearby, dense medium. Suppose that all these processes destroy a fraction  $f$  of the photons per absorption. As a photon is absorbed and re-emitted ('scattered')  $\sim \tau$  times before it eventually escapes, the plasma can still be considered effectively optically thin as long as  $f\tau \ll 1$ . The net effect on the line intensity compared to the optically thin case therefore depends on the competing processes and on the geometry. Scattering will only play a rôle in attenuating the photon line flux when there is an asymmetry in the locations of emitting and scattering region. In a stellar corona collisional de-excitation can be neglected, but scattering can re-direct photons towards the underlying, dense chromosphere where they are lost due to absorption, e.g., when the line emission occurs at the base of a scattering corona (or overlying, hot wind). For  $\tau > 1$  scattering thus results in a weakening of the line flux and the optically thin model overestimates the line flux, hence underestimates the DEM in the line-forming temperature region, leading to the generation of a hot component in the DEM so as to compensate for the underestimated continuum strength. A complication is that abundance variations and scattering have opposite effects on the line/continuum ratio: an increase in abundance leads to an increase in the line/continuum ratio but also to an increase in optical depth which leads to a reduction of this ratio.

In conclusion, with the advent of high-resolution spectrometers as *EUVE* and in future *SOHO*, *AXAF*, and *XMM*, care should be taken in the spectral fitting procedures while lines and continuum should both be used. Every DEM determination should be inspected on its individual merits taking into account (1) all the assumptions made in the spectral model and (2) considering the influence of continuum emission from plasma at temperatures where no line diagnostics is available in the relevant wavelength range.

#### REFERENCES

- ANDERS, E. & GREVESSE, N. 1989, *Geochimica et Cosmochimica Acta*, 53, 197
- BOWYER, S. & MALINA, R. F. 1991, in *Extreme Ultraviolet Astronomy*, ed. R.F. Malina & S. Bowyer, New York: Pergamon Press, 397
- CRAIG, I. J. D. & BROWN, J. C. 1986, *Inverse Problems in Astronomy*, Adam Hilger Ltd.
- DRAKE, S. A., SINGH, K. P., WHITE, N. E. & SIMON, T. 1994, *ApJ*, 436, L87
- DUPREE, A. K., BRICKHOUSE, N. S., DOSCHEK, G. A. ET AL., 1993, *ApJ*, 418, L41
- KAASTRA, J. S. & MEWE, R. 1993, *Legacy*, 3, 16
- LEMEN, J. R., MEWE, R., SCHRIJVER, C. J. & FLUDRA, A. 1989, *ApJ*, 341, 474
- MEWE, R. & KAASTRA, J. S. 1994, *European Astron. Soc. Newsletter*, Issue 8, 3
- MEWE, R., GRONENSCHILD, E. & VAN DEN OORD, G. 1985, *A&AS*, 62, 197
- MEWE, R., KAASTRA, J. S., SCHRIJVER, C. J. ET AL., 1995, *A&A*, 296, 477
- MEWE, R., LEMEN, J. R. & VAN DEN OORD, G. H. J. 1986, *A&AS*, 65, 551
- PRESS, W. H., TEUKOLSKY, S. A., VETTERLING, W. T. & FLANNERY, B. P. 1992, *Numerical Recipes*, Cambridge University Press
- RUCINSKI, S. M., MEWE, R., KAASTRA, J. S. ET AL., 1995, *ApJ*, in press
- RUMPH, T., BOWYER, S., & VENNES, S. 1994, *AJ*, 107, 2108
- SCHRIJVER, C. J., MEWE, R., VAN DEN OORD, G. H. J. ET AL., 1995, *A&A*, in press
- STERN, R. A., LEMEN, J. R., SCHMITT, J. H. M. M. ET AL., 1995, *ApJL*, in press
- SYLWESTER, J., SCHRIJVER, J. & MEWE, R. 1980, *Solar Phys.*, 67, 285
- THOMPSON, A. M. 1991, In *Intensity Integral Inversion Techniques: a Study in preparation for the SOHO Mission*, ed. R.A. Harrison & A.M. Thompson, Rutherford Appleton Lab. Rep. RAL-91, 18
- WITHBROE, G. L. 1975, *Solar Phys.*, 45, 301